Proceedings of the 2005 IEEE
International Conference on Robotics and Automation
Barcelona, Spain, April 2005

Gait Planning of Quadruped Walking and Climbing Robot for Locomotion in 3D Environment

Hyungseok Kim, Taehun Kang, Vo Gia Loc and Hyouk Ryeol Choi
School of Mechanical Engineering, Sungkyunkwan University Chunchun-dong 300, Jangan-gu, Suwon, Kyunggi-do, Korea, 440-746, hrchoi@me.skku.ac.kr

***Abstract* - One of the traditional problems in the walking and climbing robot moving in the 3D environment is how to negotiate the boundary of two plain surfaces such as corners, which may be convex or concave. In this paper a practical gait planning algorithm in the transition region of the boundary is proposed in terms of a geometrical view. The trajectory of the body is derived from the geometrical analysis of the relationship between the robot and the environment. And the position of each foot is determined by using parameters associated with the hip and the ankle of the robot. In each case of concave or convex boundaries, the trajectory that the robot moves along is determined in advance and the foot positions of the robot associated with the trajectory are computed, accordingly. The usefulness of the proposed method is confirmed through simulations and demonstrations with a walking and climbing robot.**

Keywords: Walking Robot, Climbing Robot, Quadruped, Slope, MRWALLSPECT III

I. INTRODUCTION

Up to now, applications of robots have been continuously addressed for the maintenance activities of industrial utilities such as nuclear plants, oil refineries, chemical plants, buildings, bridges, etc. The works for the aforementioned applications, in general, accompany hazardous environmental conditions as well as difficulties in access. The walking robot can be suggested as one of the solutions to cope with these situations and as illustrated in Fig. 1, it is required to possess the capability of traveling in 3D environments, different from the plain walking robots. Assuming that the environments are composed of primitive geometrical shapes, the robot should be able to move on various types of environments, such as ground to wall, wall to wall and wall to ceiling, etc. Thus the robot is required to walk as well as climb on the wall with dedicated adhesion tools such as suction, magnetic foot etc., and advanced gait planning algorithms are needed for controlling the robot.

Not so many researches have been studied on this subject up to now, even though there are numerous on the gait planning of the quadruped walking robot in the plain surfaces. Hirose et al. have addressed algorithms that generate trajectories of a body and foot positions in the horizontal plain and efficient gait planning algorithm applicable to walking on the slope and the wall considering the effect of gravity [1-5]. Shaoping et al. have proposed an algorithm to generate free gait combined with the trajectory of the body in 3D terrain [6-8]. Mohammed et al. have studied a walking algorithm and the mechanism of the robot to walk in the general terrain consisting of horizontal, inclined and vertical plain [9]. Alsalam et al. have studied transition gait from the horizontal plain to the vertical one [10]. Junmin et al. have proposed a transition gait to walk from one slope to another slope and proposed a method of estimation for the turning angle of the body [11][12].

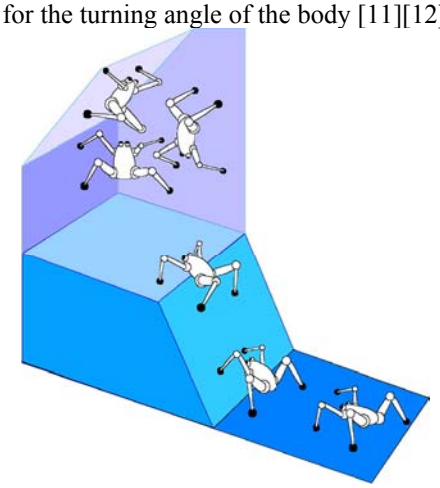

Fig. 1. Navigation in 3D environment

In this paper, assuming that the 3D environment is simplified as the combinations of primitive geometrical shapes such as plain surfaces, corners etc., a comprehensive gait planning algorithm for locomotion in the 3D environment is proposed. It is addressed how to generate appropriate trajectories of the body for moving on the concave and convex slope, and the method of determining the positions of feet in accordance with the movement of the body. Simulations are carried out and experiments are performed with a wall climbing robot called MRWALLSPECT III as shown in Fig.2[13].

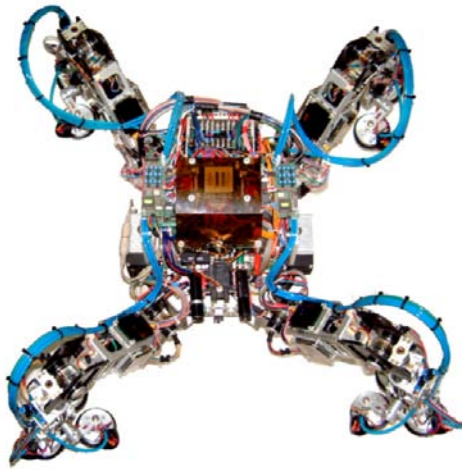

Fig. 2 MRWALLSPECT III

2. MODELS OF ROBOT AND ENVIRONMENT

As depicted in Fig. 3, the leg of MRWALLSPECT III consists of three links, whose lengths are denoted as L_1, L_2, and L_3, respectively. The ankle is a passive joint capable of producing roll, pitch and yaw motions. A frame Σ_L, called "leg frame" is located in the thigh of the leg and each axis is established as shown in Fig.3. The height of the foot h_f is defined as the distance from the bottom of the suction pad to the ankle. Since the position of the foot is determined by controlling the position of the ankle, the workspace of the leg corresponds to the area that the ankle can reach in the zx plain of Σ_L. The reachable range of the ankle is expressed as the torus with the radius of Υ such as

$$(\sqrt{x^2+y^2}-\mathrm{L}_1)^2+z^2=\Upsilon^2 \qquad (1)$$

where Υ is distance between the second joint from Σ_L and the ankle. x, y and z are coordinate values of the ankle in Σ_L. As shown in Fig. 3 the body frame Σ_B which is located in the middle of rear hip joints and the center of the front body is denoted as F_B. The length of the body is denoted as X_f and the width of the front body and the rear body is represented with Y_f and Y_r, respectively.

The pose shown in Fig. 3 is the basic configuration that the robot repeats the every gait during locomotion. Two parameters of the basic configuration, Υ of each leg and the distance h between O_B that is the origin of Σ_B and the plain the ankle has contact with, are utilized as reference values in the gait planning.

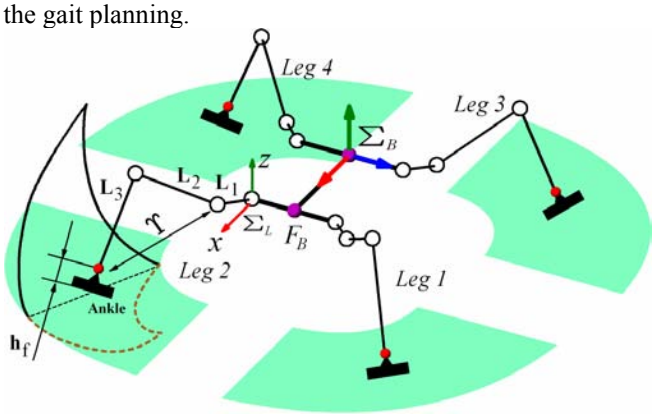

Fig. 3. Assignment of Body Coordinate Frame and Workspace

The transformation matrices from Σ_B to Σ_{Lj} (j=1,2,3,4 denotes the number of the legs) are written by

$$ {}^{B}_{L1}T=\begin{bmatrix}1&0&0&X_f\\0&1&0&\frac{Y_f}{2}\\0&0&1&0\\0&0&0&1\end{bmatrix} \quad {}^{B}_{L2}T=\begin{bmatrix}1&0&0&X_f\\0&-1&0&-\frac{Y_f}{2}\\0&0&1&0\\0&0&0&1\end{bmatrix} \quad (2) $$

$$ {}^{B}_{L3}T=\begin{bmatrix}-1&0&0&0\\0&1&0&\frac{Y_r}{2}\\0&0&1&0\\0&0&0&1\end{bmatrix} \quad {}^{B}_{L4}T=\begin{bmatrix}-1&0&0&0\\0&-1&0&-\frac{Y_r}{2}\\0&0&1&0\\0&0&0&1\end{bmatrix} $$

3D environment in this paper is simplified as combinations of plain surfaces, corners etc., which can include convex or convex corners, wall, cliff. Although there are curved surfaces or arbitrary shapes, they may be approximated as the patches of plain surfaces in the view of the robot. To make the problem easy of handling, it is assumed that the direction of movements is perpendicular to the boundary of the slope and x-direction of Σ_B is aligned with the direction of the movement. Thus, the problems in 3D environment can be treated as that of 2D environment. Let Π_{1f} be the first plain that the foot of the robot is located in and Π_{2f} be the successive plain that the foot of the robot will move on. Then, the equations of the planes represented with respect to the body frame Σ_B are written by

$$\Pi_{1f}: x\sin\gamma_1+z\cos\gamma_1=\eta_{1f} \qquad (3)$$

$$\Pi_{2f}: x\sin\gamma_2+z\cos\gamma_2=\eta_{2f} \qquad (4)$$

Here, γ_1 and γ_2 are the inclination angles of Π_{1f} and Π_{2f} with respect to the x-direction of Σ_B, respectively. η_{1f} and η_{2f} are the oriented distances from the origin of Σ_B to the planes Π_{1f} and Π_{2f} respectively. As the position of the foot is determined by controlling the position of the ankle, it is more convenient to set virtual plains Π_1 and Π_2 that run parallel with the planes Π_{1f} and Π_{2f} apart from the foot height h_f. Consequently, Eqs. (3) and (4) are converted into the equations for the planes Π_1 and Π_2 such as

$$\Pi_1: x\sin\gamma_1+z\cos\gamma_1=\eta_1 \qquad (5)$$

$$\Pi_2: x\sin\gamma_2+z\cos\gamma_2=\eta_2 \qquad (6)$$

where η_1 and η_2 are obtained by adding η_{1f} and η_{2f} with h_f, respectively.

3. Gait Planning Algorithm

The gait planning is conducted via two steps. In the first step the location of the body frame Σ_B after one cycle of gait is computed, which is denoted as Σ_N. In the second, the position of the foot is determined. Here, we set the moving distance of the robot per gait as t_p and Σ_N is calculated by applying t_p to the trajectory of the body. After obtaining Σ_N the positions of the foot are computed.

3.1 Determination of Body Trajectory

The body trajectory should be generated differently depending on the environmental conditions, that is, concave and convex environment. In the proposed method, the body trajectory is regarded as the combination of lines and arcs as shown in Figs.4 and 5. The equations of lines are easily obtained because the location of body frame is regarded apart by distance h from Π_{ih} along z-*axis* in Σ_B. Thus, the equation of the lines that the body frame moves, Π_{1h} and Π_{2h} are expressed as

$$\Pi_{1h}: x\sin\gamma_1+z\cos\gamma_1=\eta_1+h \qquad (7)$$

$$\Pi_{2h}: x\sin\gamma_2+z\cos\gamma_2=\eta_2+h \qquad (8)$$

The linear trajectory of the body Π_{1h} and Π_{2h} should be smoothed by a curve which is necessary to prevent the abrupt change of the motion of the robot. In the proposed idea, an arc is introduced as the curve. The radius of arc is determined by γ, η, d. Here, γ is the angle between the slope and the x-axis about y-axis in Σ_B and d is marginal distance between the ankle and the boundary line of Π_1 and Π_2 when the transition gait is started or completed. The relation of γ_1, γ_2 and γ is as follows:

$$\gamma = \gamma_2 - \gamma_1 \qquad (9)$$

Eqs. (10) and (11) describe the radius R of the arc of body trajectory in the concave and convex slope, respectively.

$$R = \frac{d}{\tan\frac{\gamma}{2}} - h \qquad (10)$$

$$R = \frac{d}{\tan\frac{\gamma}{2}} + h \qquad (11)$$

Figs. 4 and 5 show the body trajectory of the concave and convex slope respectively. P_S is the starting point of the transition gait and P_E is the end point of the transition gait. The transition gait begins when F_B and P_S coincide and is completed on the condition that O_B meets P_E.

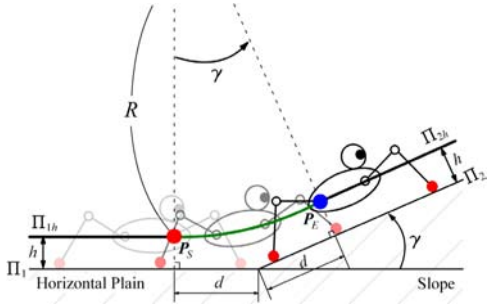

Fig. 4. Body trajectory for concave slope

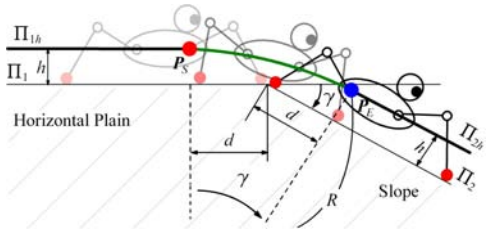

Fig. 5. Body trajectory for convex slope

In the concave transition gait, the situations are classified into four cases when O_B and F_B moves along the body trajectory. As shown in Fig. 6, case **I** is the situation that O_B is on Π_{1h} and F_B is on the arc. The position of O_N which is the origin of Σ_N is determined by Eq. (12). If $\| \boldsymbol{P}_S \|$ is less than t_p, P_S is located on O_N. F_N that is the center of the front body in Σ_N is determined whether on

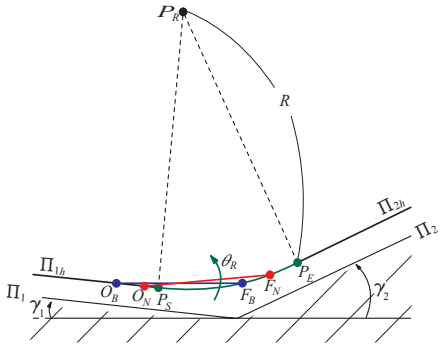

Fig. 6. Case **I** of concave transition

the arc or Π_{2h} by comparing $\| \boldsymbol{P}_E - \boldsymbol{O}_N \|$ with X_f. When $\| \boldsymbol{P}_E - \boldsymbol{O}_N \|$ is bigger than X_f, F_N on the arc is estimated by the condition of Eq. (13) or as shown in case **II** of Fig. 7, F_N on Π_{2h} is estimated by the condition of Eq. (14).

$$\boldsymbol{O}_N = t_p \frac{\boldsymbol{P}_S}{\|\boldsymbol{P}_S\|} \qquad (12)$$

$$\|\boldsymbol{F}_N - \boldsymbol{P}_R\| = R \quad , \quad \|\boldsymbol{F}_N - \boldsymbol{O}_N\| = X_f \qquad (13)$$

$$\boldsymbol{F}_N \cdot \mathbf{n}_{2h} = \eta_2 + h \quad , \quad \|\boldsymbol{F}_N - \boldsymbol{O}_N\| = X_f \qquad (14)$$

where $\mathbf{n}_{2h}$ is the normal vector of Π_{2h},

$$\mathbf{n}_{2h} = \begin{bmatrix} \sin\gamma_2 & 0 & \cos\gamma_2 \end{bmatrix}^{\mathrm{T}}.$$

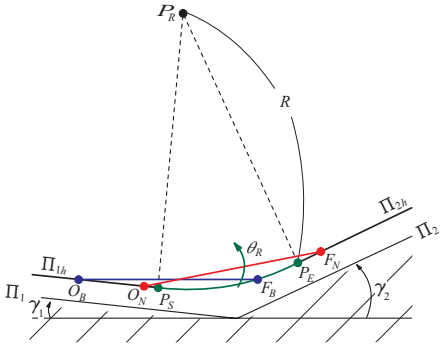

Fig. 7. Case **II** of concave transition

θ_R, the orientation angle of Σ_N is the rotation angle about *y-axis* and estimated by Eq. (15).

$$\theta_R = \operatorname{atan2}\left((\boldsymbol{F}_N - \boldsymbol{O}_N)\cdot\hat{i},\ (\boldsymbol{F}_N - \boldsymbol{O}_N)\cdot\hat{k} \right) - \frac{\pi}{2} \qquad (15)$$

where $\hat{i} = \begin{bmatrix} 1 & 0 & 0 \end{bmatrix}^{\mathrm{T}}$ and $\hat{k} = \begin{bmatrix} 0 & 0 & 1 \end{bmatrix}^{\mathrm{T}}$

In the cases **III** and **IV** shown in Figs. 8 and 9, O_N is determined by being moved from O_B with t_p along the arc. If the arc length from O_B to P_E is less than t_p, O_N is P_E. The position vector $\boldsymbol{O}_N$ is estimated by being rotated from O_B with θ_p of Eq.(16) centering around $\boldsymbol{P}_R$, the position vector of P_R. The result is found in Eq.(17).

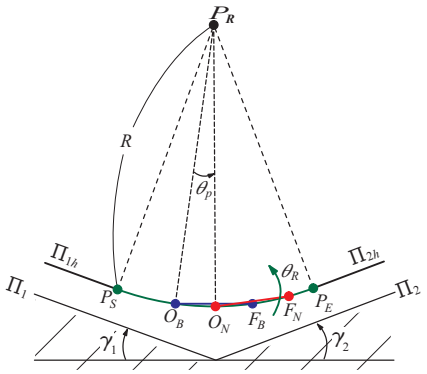

Fig. 8. Case **III** of concave transition

$$\theta_p = -\frac{t_p}{R} \qquad (16)$$

$$\boldsymbol{O}_N = \boldsymbol{P}_R + \boldsymbol{R}_Y(\theta_p)(-\boldsymbol{P}_R) \qquad (17)$$

where $\boldsymbol{R}_Y(\theta_p)$ is the rotation matrix about *y-axis*.

As θ_R is equal to θ_p in the case **III**, $\boldsymbol{F}_N$ is estimated by adding $X_f \hat{i}$ rotated by $\boldsymbol{R}_Y(\theta_p)$ to $\boldsymbol{O}_N$ as shown in Eq. (18).

$$\boldsymbol{F}_N = \boldsymbol{O}_N + X_f \cdot \boldsymbol{R}_Y(\theta_p)\hat{i} \qquad (18)$$

$$\theta_R = \frac{t_p}{R} \qquad (19)$$

where R is calculated in Eq. (11). In the case of **IV** as shown in Fig.9, $\boldsymbol{F}_N$ is found in Eq. (14) and θ_R is found in Eq. (15). In the convex transition, the case considered is only one shown in Fig. 9. O_N and F_N are determined by interior division ratio of X_f with $|\mathrm{g}_1 - \theta_R|$ and $|\mathrm{g}_2 - \theta_R|$. The interior division point P_{T2} is estimated by being moved with t_p along arc from P_{T1} which divides $\overline{O_B F_B}$ with $|\mathrm{g}_1|$ and $|\mathrm{g}_2|$ ratio interiorly.

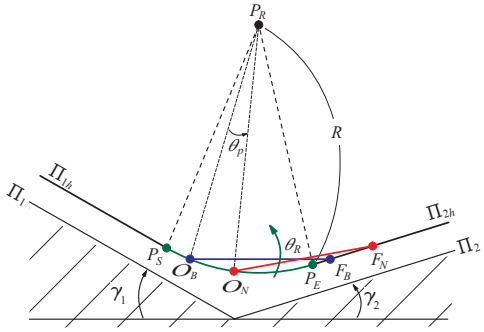

Fig. 9. Case **IV** of concave transition

The position vector $\boldsymbol{P}_{T1}$ is $\left[X_f \frac{\gamma_2}{\gamma} \quad 0 \quad 0\right]^{\mathrm{T}}$ and $\boldsymbol{P}_{T2}$ is estimated by being rotated by θ_R of Eq. (19) from $\boldsymbol{P}_{T1}$ centering around $\boldsymbol{P}_R$, the position vector of the arc center in Eq. (20). $\boldsymbol{O}_N$ and $\boldsymbol{F}_N$ are found in Eq. (21).

$$\boldsymbol{P}_{T2} = \boldsymbol{P}_R + \boldsymbol{R}_Y(\theta_R)\boldsymbol{P}_{T1} \qquad (20)$$

where

$$\boldsymbol{P}_R = \boldsymbol{P}_{T1} - R\hat{k}$$

$$\boldsymbol{O}_N = \boldsymbol{P}_{T2} - \frac{|\gamma_2 - \theta_R|}{\gamma} X_f \cdot \boldsymbol{R}_Y(\theta_R)\ \hat{i}$$

$$\boldsymbol{F}_N = \boldsymbol{O}_N + X_f \cdot \boldsymbol{R}_Y(\theta_R)\ \hat{i} \qquad (21)$$

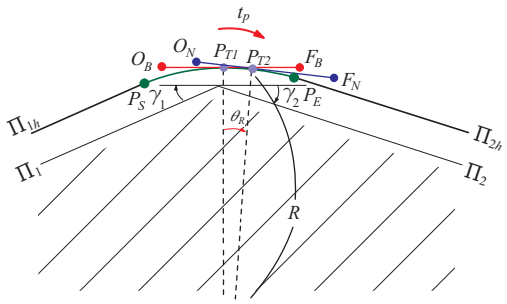

Fig. 10. Case of convex transition

In convex transition gait shown in Fig.10, the collision between the bottom of the body of the robot and the boundary edge of convex slope must be considered. Let B_t be the distance between *xy* plain of S_B and the bottom of robot body and h_m be the distance between *xy*-plain of the body of the robot and the boundary edge of the slope, then it is clear that h_m must be greater than B_t in order to avoid collision. Fig.11 describes the instance that h_m has minimum value is shown in Fig. 11. In this position, $|\mathrm{g}_1|$ and $|\mathrm{g}_2|$ are equal and the workspace of each leg has to have intersected area with P_i (i=1 to rear legs, i=2 to front legs). h_m is found in Eq. (22) and when h is fixed, the condition is satisfied by adjusting d.

$$h_m = R - \left(\frac{d}{\tan\frac{\gamma}{2}} - h_f\right)\sqrt{1+\frac{d^2}{r^2}} \qquad (22)$$

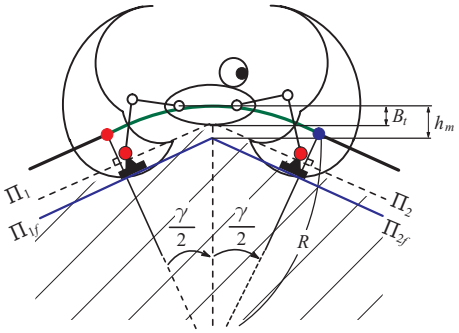

Fig. 11. Collision in convex corner

3.2 Foot Position in Leg Frame

To determine the foot position, let ${}^{Lj}\boldsymbol{P}_j$ be the foot position in S_{Lj}. ${}^{Lj}\boldsymbol{P}_j$ is on the walking plain ${}^{Lj}\prod_i$ which is inclined by g_i about *y-axis* in S_{Lj}. And let S_i be the frame whose *xy* plain is coincident with ${}^{Lj}\prod_i$ and the origin of S_i

is located from the origin of S_{Lj} by $|\eta_i|\mathbf{n}_i$ and its *y-axis* is parallel with *y-axis* of S_{Lj}. Let ${}^{i}\boldsymbol{P}_j$ be the description of ${}^{Lj}\boldsymbol{P}_j$ in S_i, then the relation of ${}^{Lj}\boldsymbol{P}_j$ and ${}^{i}\boldsymbol{P}_j$ is described in Eq. (23).

$$ {}^{Lj}\boldsymbol{P}_j = {}^{Lj}_{i}\boldsymbol{T}\ {}^{i}\boldsymbol{P}_j \qquad (23) $$

where

$$ {}^{Lj}_{i}\boldsymbol{T} = \begin{bmatrix} \boldsymbol{R}_Y(\gamma_i) & |\eta_i|\mathbf{n}_i \\ 0\ 0\ 0 & 1 \end{bmatrix} $$

From Eqs. (1) and (23) with setting ${}^{i}z_j = 0$, we have the workspace area of the leg on S_W as follow.

$$ {}^{i}x_j^{\,2} + {}^{i}y_j^{\,2} + 2\mathrm{L}_1\sqrt{{}^{i}x_j\cos\gamma_i + \eta_i\sin\gamma_i} = \Upsilon^2 - \mathrm{L}_1^{\,2} - \eta_i^{\,2} \quad (24) $$

${}^{i}\boldsymbol{P}_j$ is determined by giving ${}^{i}y_j$ which is equal to ${}^{Lj}y_j$ and ${}^{Lj}\boldsymbol{P}_j$ is estimated by Eq. (23).

3.3 Synthesis of Body and Foot Position

The foot position $\boldsymbol{P}_j$ in S_B associated with the body trajectory is estimated by the following steps. First, ${}^{N}\prod_i$ which is the description of P_i in S_N is estimated and transformed to ${}^{Lj}\prod_i$ (i=1 for j=3,4 and i=2 for j=1,2) which is the description of ${}^{N}\prod_i$ of each leg frame in Eq. (2). By applying the foot position determination algorithm to ${}^{Lj}\prod_i$, ${}^{Lj}\boldsymbol{P}_j$, jth foot position, is determined in S_{Lj}. By Eq. (2), ${}^{N}\boldsymbol{P}_j$ is estimated from ${}^{Lj}\boldsymbol{P}_j$ and finally $\boldsymbol{P}_j$ is found by transforming ${}^{N}\boldsymbol{P}_j$ into S_B.

4. SIMULATIONS

The proposed algorithm was tested by simulation with parameters of MRWALLINSPECT III. The simulation was carried out for two cases. The one is climbing up the hill with 35 degrees of the slope and the other is the going down the hill. In both cases, concave and convex transition gait are performed sequentially. Figs. 12 and 13 show the concave and convex transition of climbing up hill respectively. In *Side 3* of Fig. 13, it is observed that the bottom of the body collides with the boundary edge of P_f which is displayed as the lower plain. Figs. 14 and 15 show the convex and concave transition of going down hill respectively. Obviously, it is observed that the bottom of the body collides with the boundary edge of P_f which is displayed as the lower plain in *Side 3* of Fig. 14. Consequently, it can be concluded that the bottom of the body and the boundary edge of convex slope are not collide with by applying condition of h_m in Eq. (22).

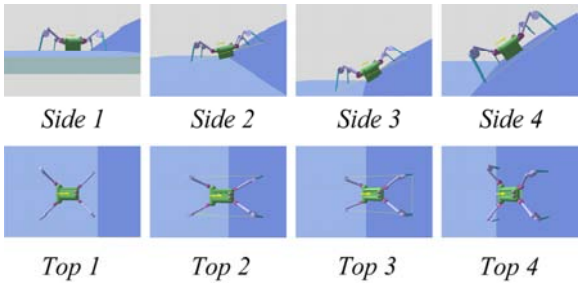

Fig. 12. Climbing up concave slope

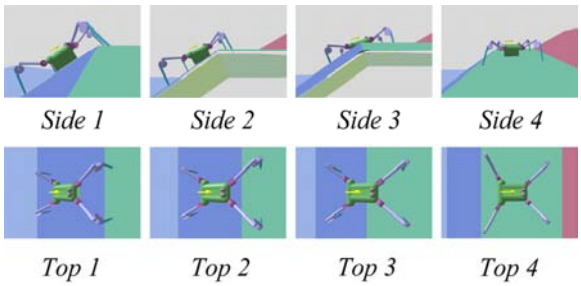

Fig. 13. Climbing up convex slope

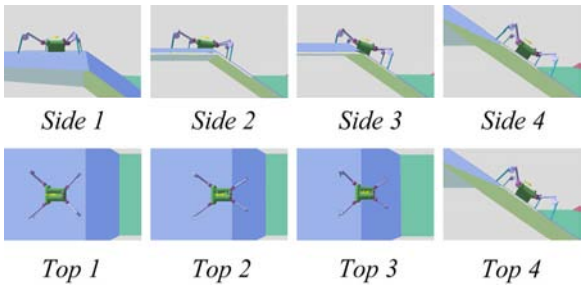

Fig. 14. Going down convex slope

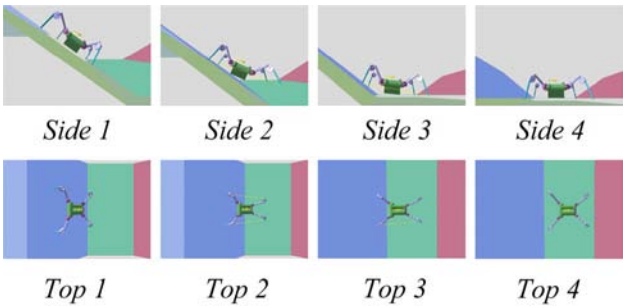

Fig. 15. Going down concave slope

5. EXPERIMENTS

In the experiments, the validity of the proposed algorithms has been demonstrated using a walking robot, called MRWALLSPECT III [13]. MRWALLSPECT III has been developed for walking and climbing in 3D environments. Climbing over a slope with concave corner was tested as shown in Fig. 16. When the robot moves up or down on the slope, tumbling of the robot and slipping of the legs should be avoided. However, in the case of the walking robot with suction pads, these problems may be neglected because the legs always have adhesive forces between the ground and the legs. The *step 1* of Fig. 16 shows the approach phase for the transition gait in the slope.

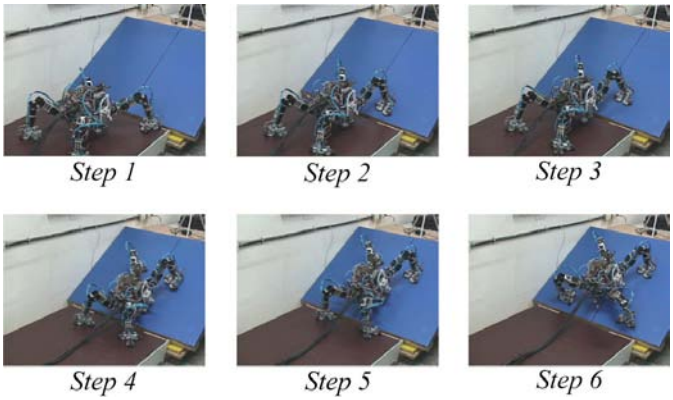

Fig. 16. Concave transition gait

In this case, the slope angle measured was approximately 35 degrees. And, the *step 2* and *step 3* describe the transition in the concave corner. In the last step, the robot climbs over the slope with plain surfaces using climbing gait.

6. Conclusion

In this paper, we proposed a gait planning algorithm for a quadruped walking and climbing robot to negotiate the boundary region between two plains. First, we determine the body trajectory in which the robot has to trace and suggest a method of determining the foot position associated with the body trajectory in terms of the body frame of the robot. Also, we explain the possibility condition of the convex transition gait. Through simulations and experiments, the effectiveness of the proposed algorithm has been proved.

Acknowledgment

The authors are grateful for the support provided by a grant from the Korea Science & Engineering Foundation(KOSEF) and the Safety and Structural Integrity Research Center at the Sung Kyun Kwan University.

References

[1] Shigeo Hirose, Hidekazu Kikuchi and Yoji Umetani, "The Standard circular gait of a quadruped walking vehicle", *Advanced Robotics*, Vol. 1, No. 2, pp. 143-164, 1986.

[2] Shigeo Hirose, Yasushi Fukuda and Hidekazu Kikuchi, "The gait control system of a quadruped walking vehicle", *Advanced Robotics*, Vol. 1, No. 4, pp. 289-323, 1986.

[3] Shigeo Hirose and Kazuhito Yokoi, "The standing posture transformation gait of a quadruped walking vehicle" *Advanced Robotics*, Vol. 2, No. 4. pp. 345-359, 1988.

[4] Keisuke Arikawa and Shigeo Hirose, "Study of Walking Robot for 3 Dimensional Terrain (optimization of walking motion based on GDA and Coupled Drive)", *Proc. of IEEE Int. Conf. on Robotics and Automation*, pp. 703-708, 1995.

[5] Hideyuki Tsukagoshi, Shigeo Hirose and Kan Yoneda, "Maneuvering Operations of the Quadruped Walking Robot on the Slope", *Proc. of IEEE/RSJ Int. Conf. on Intelligent Robots and Systems*, pp. 863-869, 1996.

[6] Shaoping Bai, K. H. Low and Teresa Zielinska, "Quadruped free gait generation combined with body trajectory planning", *Proc. of the First Workshop on Robot Motion and Control*, pp. 165-170, 1999.

[7] Shaoping Bai and K. H. Low, "Body Trajectory Generation for Legged Locomotion Systems Using A Terrain Evaluation Approach", *Proc. of IEEE Int. Conf. on Robotics and Automation*, pp. 279-2284, 2001.

[8] Shaoping Bai, K. H. Low and Teo M. Y, "Path generation of walking machines in 3D terrain", *Proc. of IEEE Int. Conf. on Robotics and Automation*, pp. 2216-2221, 2002.

[9] Mohammed Yassir Al- Zaydi and Shamsudin H. M. Amin, "Locomotion Simulation of A quadruped Robot on General Level Terrain", *Proc. of IEEE Int. Conf. on Intelligent Engineering Systems*, pp. 159-164, 1997.

[10] Abd Alsalam Sh. I. Alsalameh, Shamsudin H. M. Amin and Rosbi Mamat, "Mechanical Design of A Quadruped Robot for Horizontal Ground to Vertical Wall Movement", *Proc. of TENCON 2000*, pp. 213-217, 2000.

[11] Jummin Pan and Junshi Cheng, "Study of quadruped walking robot climbing and walking down slope", *Proc. of IEEE/RSJ Int. Conf. on Intelligent Robots and Systems*, pp. 1531-1534, 1991.

[12] Junmin Pan and Junshi Cheng, "Gait Synthesis For Quadruped Robot Walking Up and Down Slope", *Proc. of IEEE/RSJ Int. Conf. on Intelligent Robots and Systems*, pp. 532-536, 1993.

[13] Taehun Kang, Hyungseok Kim, Taeyoung Son and Hyoukryeol Choi, "Design of Quadruped Walking and Climbing Robot", *Proc. of IEEE/RSJ Intelligent Robots and Systems*, pp. 619-624, 2003.